JP1.2

ESTIMATING SURFACE HEAT FLUXES AND RELATED PARAMETERS BY COMBING SATELLITE BRIGHTNESS TEMPERATURE AND A HEAT BUDGET MODEL OVER A SEMI-ARID STEPPE

Dai Matsushima *
Chiba Institute of Technology, Narashino, Chiba, Japan

1. Introduction

In a semi-arid area, evapotranspiration over the land surface plays a critical role not only in the water circulation over that surface, and also in many associated physics and ecology aspects. This study estimates the temporal change and spatial distribution of evapotranspiation and other components of the surface heat budget over a semi-arid steppe, the Kherlen River Basin in Mongolia in a growing season of vegetation. The landscape in this region sequentially changes from forest in the northern part, to forest steppe, typical steppe, and finally dry steppe southward. This landscape change influences, and is influenced by, regional water conditions, and a precise estimate of the temporal and spatial distributions of evapotranspiration is important for determining local and regional water budgets in and around this region. This paper is divided into two themes as follows: (1) A temporal change of a local surface heat fluxes in the Kherlen River Basin over a growing season (May through October in year 2003), and (2) The spatial distribution of surface heat fluxes of a few days in the growing season over the Kherlen River Basin where the local point examined in (1) is included. This study also investigates the development of a technique to estimate surface heat fluxes, incorporating satellite data into a numerical model of surface heat budget. This kind of estimation of surface heat fluxes has been developed for a few decades, and recently several methods incorporating satellite data, especially thermal-infrared data, into numerical surface heat budget models have been proposed (Caparrini et al., 2004; Crow and Kustas, 2005; Demarty et al., 2004). Our study proposes a different procedure to retrieve parameters with regard to the heat transfer, employing the simplex algorithm incorporated into a two-layer model modified into the force-restore form. This model was originally developed by Matsushima and Kondo (1995) for estimating heat transfer over a bare soil surface, and is modified in this study using a two-layer model developed by Kondo and Watanabe (1992).

* Corresponding Author Address: Dr. Dai Matsushima, Chiba Institute of Technology, 2-17-1 Tsudanuma, Narashino, Chiba, 275-0016 Japan; e-mail: matsushima.dai@it-chiba.ac.jp

2. Materials and Methods

2.1 *Methods*

Figure 1 schematically illustrates the flow for estimating the spatial distribution of surface heat fluxes, incorporating remote sensing data into a surface heat budget model in this study. The flow consists of data sources, data processing, input data, data used for parameter optimization, and results. A thermal infrared band of the Moderate Resolution Imaging Spectroradiometer (MODIS) provides brightness temperature at the satellite level, which is modified to brightness temperature at the Earth’s surface through atmospheric correction. The geostationary satellite, GOES-9, provides reflectance of visible, near-infrared, and thermal-infrared bands that are processed to retrieve incoming solar radiation $S^{\downarrow}$. Surface meteorological data (air temperature T_a, specific humidity q, and wind speed U) are provided by routine meteorological stations, which are also used for estimating downward longwave radiation $L^{\downarrow}$. The bulk parameters in the heat budget model

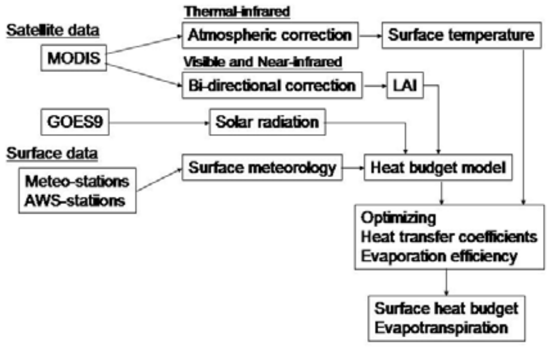

Fig. 1 Schematic of the flow from data to final results.

with regard to the turbulent heat and water vapor transfer are optimized in the model using the surface brightness temperature. The linear heat budget model is a combination of the heat budget equation on the Earth's surface and the bulk formulas of turbulent transfer of heat and water vapor. This model calculates temporal changes of surface temperatures of the subsurface soil and the vegetation canopy, which are denoted by T_g and T_c, given a time series of input variables, $S^{\downarrow}$, $L^{\downarrow}$, T_a, q, and U. Finally, the calculated time series of surface temperatures can reproduce temporal change of surface heat fluxes.

2.2 *Data*

Radiance of channel 31 of the MODIS L1B data (wavelength: 10.78 to 11.28 μm) was used for the brightness temperature, which was modified in terms of the atmospheric absorption employing the MODTRAN code incorporated with a mesoscale objective analysis data of atmosphere (20 km resolution) archived by the Japan Meteorological Agency. The linear heat budget model requires values of leaf area index (LAI) to calculate the brightness temperature of the surface at an arbitrary viewing angle. In this study, LAI was derived from the normalized difference vegetation index (NDVI) using the reflectance data of the L1B data with bi-directional reflectance correction (Matsushima et al., 2005). The grid formation employed in the model calculation was a unique one, in which the coordinate was determined by latitude and longitude and the spatial resolution was 2 km, to avoid that of MODIS L1B data changing according to individual shots. The time series of the spatial distribution of incoming solar radiation was calculated using an archive of the reflectance and thermal brightness temperature of the geostational satellite GOES-9 and the method developed by Kawamura et al. (1998) on an hourly basis. The Kawamura's method mainly considers solar flux decay due to cloud, ozone, and aerosols by simple parameterizations. The average root-mean-squares error (RMSE) was around 90 Wm^{-2} on an hourly basis, which was based on data used in this study. The spatial resolution of archive data is 0.05° both in longitude and latitude (about 5 km). The spatial resolution of the solar radiation was not reorganized as the MODIS data, but nearest neighbor values were used in the model calculation. Surface meteorological data was provided using routine meteorological stations in Mongolia (meteo-stations) operated by the Institute of Meteorology and Hydrology, one flux station (KBU-A1: 47.20N, 108.74E) and four automatic weather stations operated by the Rangelands Atmosphere-Hydrosphere-Biosphere Interaction Study Experiment in Northeastern Asia (RAISE**)** project conducted in the subject region. The data archives provide time series of air temperature, relative humidity, and wind speed at individual stations. Downward longwave radiation at the other stations was estimated by the surface meteorological data and the estimated incoming solar radiation using methods developed by Kondo and Miura (1985), and Kondo et al. (1991) to obtain daily average values of individual stations. Values of radiation, turbulent heat, and subsurface heat were supplied by data obtained at the KBU-A1 station, which is a fundamental flux station of the RAISE project over a typical steppe. The eddy-correlation flux data was used for validation of the model results.

3. Linear Surface Heat Budget Model

3.1 *Model Description*

The heat budget model used in this study mainly consists of the heat budget equation and the bulk formulation of the turbulent heat transfer on the Earth's surface. The heat budget equation on the two layers, canopy and soil surface, are formulated based on Kondo and Watanabe (1992) and given as :

$$(1-f_s)(1-a_c)S^{\downarrow}+\varepsilon_c(1-f_L)(L^{\downarrow}+\varepsilon_g\sigma T_g^4)-2(1-f_L)\varepsilon_c\sigma T_c^4-G_c = H_c+lE_c \quad (1)$$

and

$$f_s(1-a_g)S^{\downarrow}+f_L\varepsilon_g L^{\downarrow}-\varepsilon_g\sigma T_g^4+\varepsilon_g(1-f_L)\varepsilon_c\sigma T_c^4-G_g = H_g+lE_g \quad (2)$$

where subscript c denotes canopy surface and g denotes soil surface, a albedo, ε thermal emissivity, σ the Stefan-Boltzmann constant, G the subsurface heat flux, H the sensible heat, and lE the latent heat. The transmittances of radiation are estimated by parameterizations described by Ross (1975) as $f_S=\exp(-F\cdot LAI\cdot\sec\theta)$ and $f_L=\exp(-F\cdot LAI\cdot d)$, where the effective transmittance of the solar radiation of the canopy at the solar zenith angle θ and on the leaf area index LAI, and the effective transmittance of the longwave radiation of the canopy, respectively. The leaf inclination factor F was set to be 0.5 assuming that the leaf inclination of individual leaves was random (Ross, 1975), and the diffusivity factor d was set to be 1.66 assuming that the longwave radiation was isotropic. The sensible and latent heat fluxes are expressed as the bulk transfer formulations proposed in Matsushima and Kondo (1995) for the bare soil surface, which are applied to the two-layer model given as:

$$H_c=c_p\rho(C_{Hc}U_M+b_cU')(T_c-T_a) \quad (3)$$

$$lE_c=l\rho\beta_c(C_{Hc}U_M+b_cU')\left(q_s(T_c)-q_a\right), \quad (4)$$

$$H_g=c_p\rho(C_{Hg}U_M+b_gU')(T_g-T_a) \quad (5)$$

and

$$lE_g=l\rho\beta_g(C_{Hg}U_M+b_gU')\left(q_s(T_g)-q_a\right), \quad (6)$$

where C_H denotes the daily average of the bulk transfer coefficient for sensible heat, b the slope of the bulk transfer coefficient with regard to departure from the daily average wind speed U', in which the superscript $()'$ denotes the departure, while U_M represents the daily average in which the subscript M denotes the average: β the evaporation efficiency, c_p the specific heat of air at constant pressure: ρ the density of air: l the latent heat of water for evaporation: and $q_s(T)$ the saturation specific humidity at the temperature T. The subsurface heat flux under soil surface G_g is formulated using the force-restore method and is given as :

$$G_g=\frac{P_g}{\sqrt{2\omega}}\left(\frac{dT_g'}{dt}+\omega T_g'\right), \quad (7)$$

where $P_g=\sqrt{c_g\rho_g\lambda_g}$ is the subsurface thermal inertia, ω the angular velocity of diurnal change, c_g the subsurface specific heat, ρ_g the subsurface density, and λ_g the subsurface thermal conductivity. The heat storage of the canopy G_c is similarly expressed as :

$$G_c=C_c\frac{dT_c'}{dt}, \quad (8)$$

where C_c is the heat capacity of the canopy.

Substituting Eqs.(3)-(8) into Eqs.(1)-(2), and dividing the equation into components of the daily average and the diurnal change as

$T_c = T_{cM} + T_c'$, a summarized form of the equation is derived after some manipulation:

$$\frac{d}{dt}\begin{pmatrix} T_c' \\ T_g' \end{pmatrix} = A\begin{pmatrix} T_c' \\ T_g' \end{pmatrix} + B\begin{pmatrix} S^{\downarrow\prime} \\ L^{\downarrow\prime} \\ T_a' \\ q_a' \\ U' \end{pmatrix}. \qquad (9)$$

Here, A and B are coefficient matrices. The above equations describe the diurnal change of surface temperatures of two layers.

To retrieve the observable variable, which is the brightness temperature T_r , from the state variables T_c and T_g , we employ the following formula which considers a simple radiation process within the canopy and is given as:

$$\begin{aligned} T_r &= f_a \varepsilon_g T_g + (1 - f_a)\varepsilon_c T_c \\ &+ \left[(1-\varepsilon_g) f_a f_L + (1-f_a)(1-\varepsilon_c)(1-f_L)\right] T_{sky} \\ &+ \left[1 - f_a(\varepsilon_g + (1-\varepsilon_g) f_L - (1-f_a)\{\varepsilon_c + (1-\varepsilon_c)(1-f_L)\}\right] \frac{n-1}{n} T_{aM} \end{aligned} \qquad (10)$$

where $f_a = \exp(-F \cdot LAI \cdot \sec\phi)$ denotes the effective transmittance of thermal-infrared radiance formulated as the effective transmittance of the solar radiation f_s ; T_{sky} the effective temperature of the downward longwave radiation, and n is defined in a empirical formula which regresses the black body radiation in a certain range of wavelength as (black body radiation) $= kT^n$, where k is a proportional constant. The value of n was set to 4.8 after Matsushima and Kondo (1997). All variables and parameters with regard to Eq. (10) should be values corresponding to the same range of wavelength.

3.2 *Optimizing Surface Parameters*

Parameters for turbulent heat and water vapor transfer should be optimized to reasonably estimate the surface heat budget. As mentioned in the previous subsection, the bulk transfer coefficient for sensible heat C_H, the slope of the bulk coefficient *b*, the evaporation efficiency β, and the thermal inertia P_g were optimized both for soil and the canopy surface on a daily basis, except for P_g. The optimization was achieved by minimizing the difference between the estimated brightness temperature T_r calculated by Eq. (10) and the satellite brightness temperature which was atmospherically corrected. Seven or more samples of observed surface temperature are needed for optimization because there are seven parameters to be optimized. The best combination of parameters should be sought to minimize the objective function, which is the sum of the squares of the difference between the estimation and the satellite temperature. The simplex method was employed for the algorithm seeking the best combination of parameters. In this study, parameters were optimized in two ways. One is effective if an observed time series of surface temperature is available. The estimated surface temperature time series changes according to the turbulent parameters. This method is called hereafter temporal optimization. Parameters at the KBU-A1 station were determined in this way, using the diurnal change (only in daytime) of the surface brightness temperature which was transformed from the upward longwave radiation flux. In estimating the spatial distribution of surface heat fluxes, this temporal optimization is difficult to achieve because no sufficient time series of satellite brightness temperature is available. In this case, the temporal change of the surface temperature can be replaced by the spatial distribution in calculating the objective function if the number of grids exceeds the number of parameters. This method considers the fact that the surface temperature can be different from grid to grid, depending on the distribution of solar radiation and meteorological conditions, even for the neighboring grids, and is called hereafter spatial optimization. In this study, the daily average

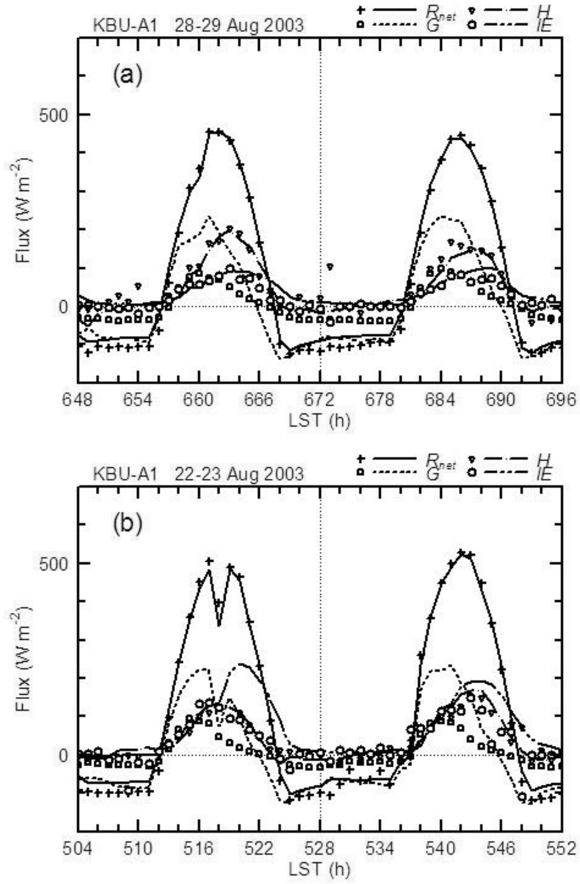

Fig. 2 Diurnal course of the heat budget components at the KBU-A1 station on (a) 28-29 August 2003 and (b) 22-23 August 2003. Lines denote estimations by temporal optimization and symbols denote observation.

of the parameters was determined for every 6 km square, which included 9 grids. The turbulent parameters were assumed to be constant inside the 6 km squares.

4. Results and Discussion

4.1 *Seasonal Change of Evapotranspiration at the KBU-A1 station*

Figure 2 illustrates comparisons of estimation and observation of the diurnal course of surface heat fluxes at the KBU-A1 station. The RMSEs in daytime (0700-2000 LST) on an hourly basis for sensible heat were 29 Wm^{-2} for 22 Aug., 25 Wm^{-2} for 23 Aug., 17 Wm^{-2} for 28 Aug., and 16 Wm^{-2} for 29 Aug. 2003, and 81 Wm^{-2}, 79 Wm^{-2}, 23 Wm^{-2},

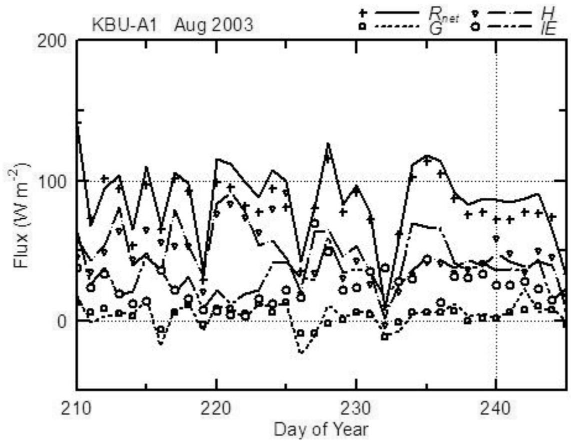

Fig. 3 Daily changes of the daily average of estimated surface heat fluxes at the KBU-A1 station in August 2003. Lines and symbols are the same as in Fig. 4.

and 15 Wm^{-2} for latent heat on the same dates. Figure 3 illustrates estimates of the daily averages of the surface heat fluxes at the KBU-A1 station in August 2003. The performance of estimation was generally good with RMSEs of 15 and 17 Wm^{-2} for sensible and latent heat in overall August, respectively, and 14 and 15 Wm^{-2} over the growing season. The daily changes of the evaporation efficiency of canopy and the thermal inertia optimized by the model are illustrated in Fig. 4, where the daily average of the volumetric soil water content (hereafter simply referred to soil moisture) at the depth of 5 cm and the daily precipitation, both of which were observed at the KBU-A1 station, are also shown. The estimated two parameters were well correlated with the soil moisture of the shallow layer. The correlation coefficients of the thermal inertia and the evaporation efficiency of canopy with the soil moisture were 0.42 and 0.49 over the whole growing season, and that of the thermal inertia with the evaporation efficiency of canopy was 0.73. This indicates changes in not only the evaporation efficiency but also the thermal inertia reflected the change in the soil moisture. The thermal inertia is a multiplication of the heat capacity and the thermal conductivity, and both monotonously increase as the soil moisture increases, in

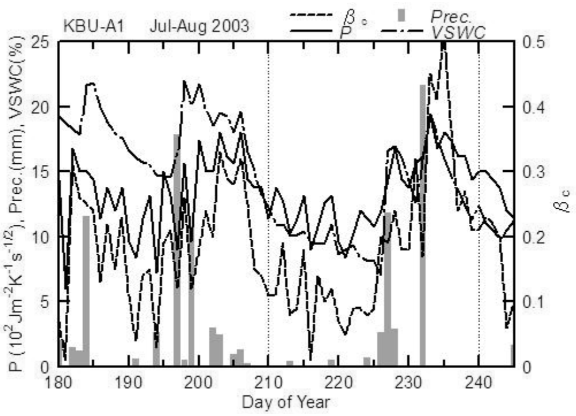

Fig. 4 Daily changes of the evaporation efficiency of canopy (β_c) and the subsurface thermal inertia (P_g) at the KBU-A1 station in July and August 2003 estimated by the model optimizations.

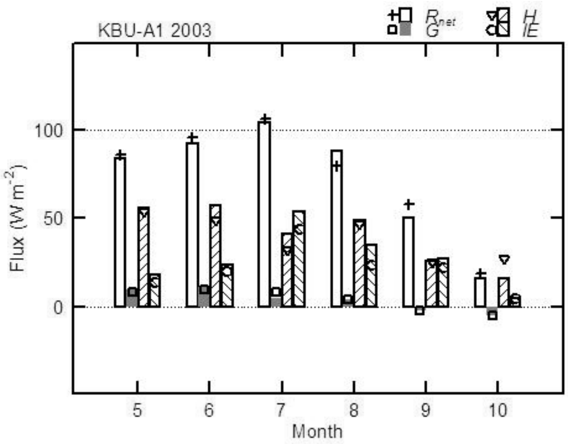

Fig. 5 Monthly average of the estimated heat budget components at the KBU-A1 station in the growing season in the year 2003. Histograms denote estimations and symbols denote observations.

particular, the thermal conductivity rapidly increases when the soil moisture is very small (Brutsaert, 1982). The soil moisture in the subject region over the growing season was mostly below 15% except July, the latter half of September, and soon after a heavy rainfall. These dry conditions are consistent with the range of the rapid change of thermal conductivity with soil moisture. Therefore, the thermal inertia should be optimized with other related parameters especially under dry conditions, and further suggests the spatial and temporal distribution of soil water conditions can be estimated by the present method. Figure 5 illustrates the monthly average of the heat fluxes over the growing season. Every estimated heat flux was comparative with the observation with the difference between the estimation and the observation being less than about 10 Wm^{-2}.

4.2 *Spatial Distribution of Evapotranspiration*

Figure 6 compares the heat fluxes and the brightness temperature between the observation at the KBU-A1 station and the estimation by the spatial optimization at the nearest grid to the KBU-A1 station. Estimates of both the heat fluxes and the brightness temperature were generally good. Figure 7 illustrates spatial distributions of the daily averages of the evapotranspiration (latent heat) on 22 and 23 August 2003 over the subject region. The blank area in the figures indicates where the surface was covered with clouds, and no surface data was available at the time. The amount of the daily evapotranspiration was mostly less than 2.5 mm day^{-1}. There were some grids where the daily evapotranspiration exceeded 3 mm day^{-1}, which does not indicate real situations because some broken clouds may have existed over these areas, and clouds lowered the satellite brightness temperature and made the estimation unreasonably larger. Excluding these questionable areas, the evapotranspiration was relatively larger in areas along Kherlen River on 22 August, where the sensible heat was small. On 23 August, the evapotranspiration was less than the previous day in most grids, especially in an area south of UDH and east of DH, where the sensible heat was about the same as the previous day. On the other hand, the evapotranspiration was about the same as the previous day in an area east of UDH, where the sensible heat was very small. There was a sufficient amount of rainfall (5-25mm) over most areas in the whole region on 20 August, and a periodic rainfall lasted until 22 August in the area east of UDH. Figure 8 illustrates distributions of

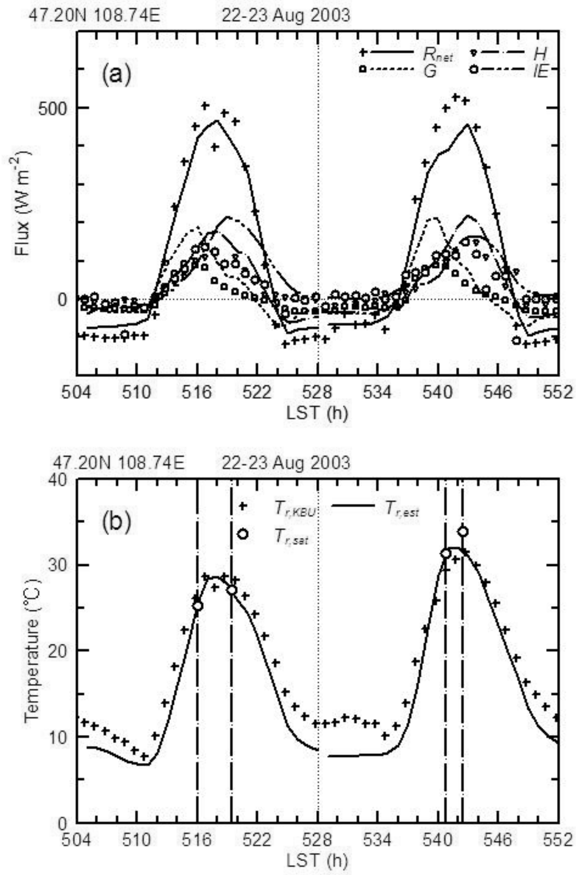

Fig. 6 Comparison of (a) the heat fluxes and (b) the brightness temperature between the observation at the KBU-A1 station and the estimation by the spatial optimization at the nearest grid (47.20°N, 108.75°E) to the KBU-A1 station. The satellite brightness temperature $T_{r,sat}$ and the surface brightness temperature $T_{r,KBU}$, and the estimation $T_{r,est}$ are shown in (b).

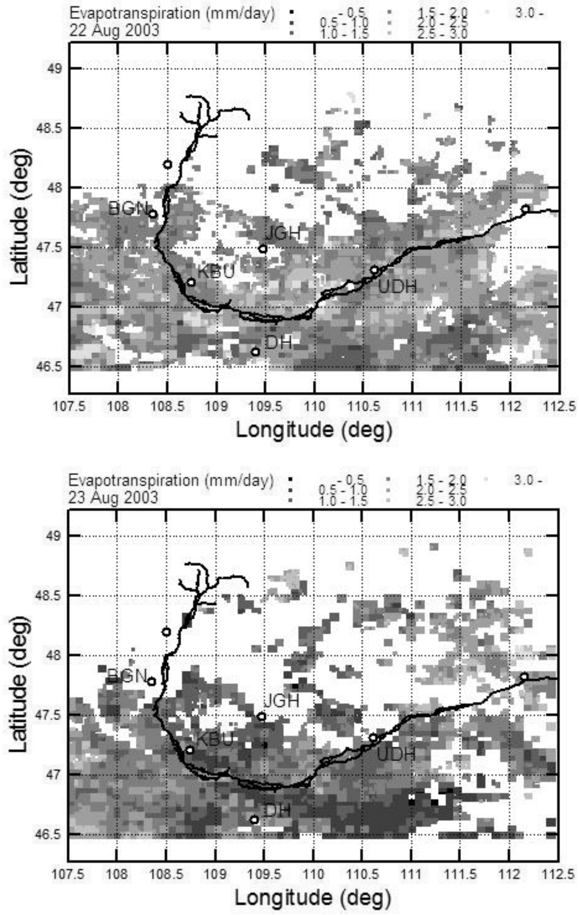

Fig. 7 Spatial distribution of the evapotranspiration on 22 and 23 August 2003 over the subject region.

and the thermal inertia, which were optimized by the model calculation. Spatial distribution of the parameter was well correlated with that of the rainfall and successive evapotranspiration.

5. Conclusion

Spatial distribution and temporal change of the surface heat fluxes over a semi-arid region were estimated by incorporating the satellite brightness temperature of the Earth's surface into a linear surface heat budget model. Surface heat fluxes were estimated by using a force-restore formed two-layer model, in which the temporal and the spatial optimization techniques and the simplex algorithm were incorporated. The flux results estimated by both the temporal and the spatial optimization were validated by the observation at a flux station located in a typical steppe. The optimized parameters also showed physical state at the surface and subsurface. In particular, the evaporation efficiency and the thermal inertia were highly correlated with the volumetric soil water content at a shallow layer. The thermal inertia should be optimized with other relevant parameters especially under dry conditions. Results of spatial distribution of the surface heat

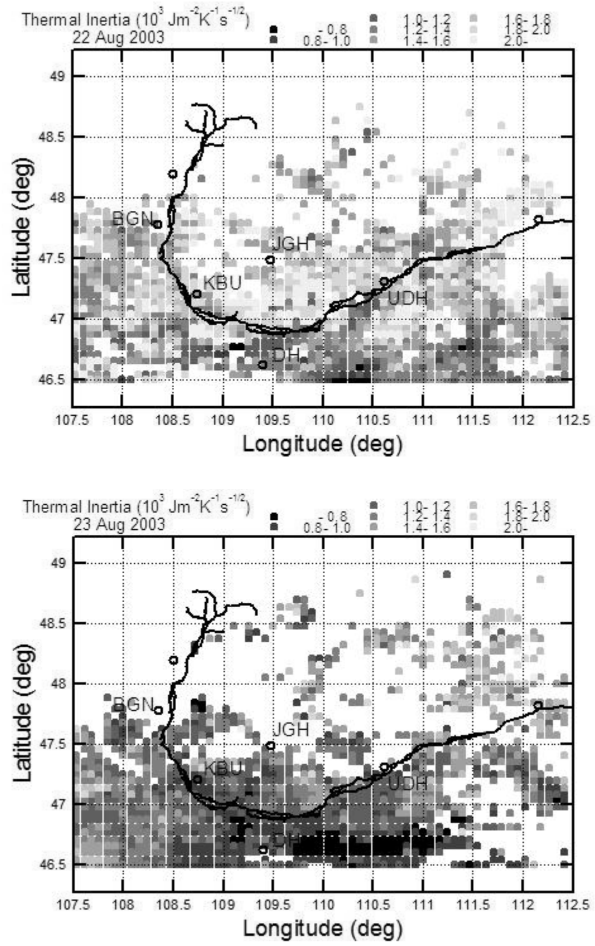

Fig. 8 Spatial distribution of the subsurface thermal inertia on 22 and23 August.

fluxes after a rainfall on successive summer days showed that estimated evapotranspiration was consistent with the amount of rainfall and a relevant parameter. This study confirmed the feasibility of estimating surface heat fluxes over a semi-arid region, especially the feasibility of the spatial optimization and the optimized thermal inertia reflecting subsurface water conditions. Future issue should be to reproduce climatology of spatial distributions of surface heat fluxes as well as subsurface water conditions over semi-arid regions.

References

Brutsaert, W.: Evaporation into the atmosphere, D. Reidel Publishing Company, 299 pp, 1982.

Caparrini, F., F. Castelli, D. Entekhabi: Variational estimation of soil and vegetation turbulent transfer and heat flux parameters from sequences of multisensor imagery, *Water Resour. Res.*, **40**, W12515, doi:10.1029/2004WR003358, 2004.

Crow, W. T. and W. P. Kustas : Utility of assimilating surface radiometric temperature observations for evaporative fraction and heat transfer coefficient retrieval, *Bound.-Layer Meteorol.*, **115**, 105-130, 2005.

Demarty, J., C. Ottle, I. Braud, A. Olioso, J. P. Frangi, L. A. Bastidas, and H. V. Gupta: Using a multiobjective approach to retrieve information on surface properties used in a SVAT model, *J. Hydro.*, **287**, 214-236, 2004.

Kawamura, H., S. Takahashi, and T. Takahashi: Estimation of insolation over the Pacific Ocean off the Sanriku Coast, *J. Oceanography*, **54**, 457-464, 1998.

Kondo, J. and A. Miura: Surface heat budget of the western pacific for May 1979, *J. Meteorol. Soc. Jpn.*, **63**, 633-646, 1985.

Kondo, J., T. Nakamura, and T. Yamazaki: Estimation of the solar and downward atmospheric radiation, *Tenki*, **38**, 41-48, 1991 (in Japanese with English abstract).

Kondo, J. and T. Watanabe: Studies on the bulk transfer coefficients over a vegetated surface with a multilayer energy budget model, *J. Atmos. Sci.*, **49**, 2183-2199, 1992.

Matsushima, D. and J. Kondo: An Estimation of the Bulk Transfer Coefficients for a Bare Soil Surface Using a Linear Model, *J. Appl. Meteorol.*, **34**, 927-940, 1995.

Matsushima, D., Y. Matsuura, I. Byanbakhuu, and Ts. Adyasuren: Estimating inter- and intra-seasonal changes of satellite NDVI and LAI over Kherlen River Basin using a bi-directional reflectance correction, *Proceedings of the first international symposium on terrestrial and climate change in Mongolia*, 137-140, 2005.

Ross, J.: Radiative transfer in plant communities, In *Vegetation and the Atmosphere 1* (ed. by J. L. Monteith), Academic Press, 13-35, 1975.